Path Constraints in Tychastic and Unscented Optimal Control: Theory, Application and Experimental Results

I. Michael Ross, Mark Karpenko, and Ronald J. Proulx

Abstract— In recent papers, we have shown that a Lebesgue-Stieltjes optimal control theory forms the foundations for unscented optimal control. In this paper, we further our results by incorporating uncertain mixed state-control constraints in the problem formulation. We show that the integrated Hamiltonian minimization condition resembles a semi-infinite type mathematical programming problem. The resulting computational difficulties are mitigated through the use of the unscented transform; however, the price of this approximation is a solution to a chance-constrained optimal control problem whose risk level is determined a posteriori. Experimental results conducted at Honeywell are presented to demonstrate the success of the theory. An order of magnitude reduction in the failure rate in obtained through the use of an unscented optimal control that steers a spacecraft testbed driven by control-moment gyros.

I. INTRODUCTION

In [1], we introduced the concept of unscented optimal control. Thereafter, we provided a theoretical framework for the technique in terms of a Lebesgue-Stieltjes optimal control theory [2]–[5]. In simple terms, unscented optimal control combines the concept of the unscented transform of Julier et al [6]–[9] with standard deterministic optimal control [10], [11] to produce an unscented approach for controlling a conditionally deterministic dynamical system. Such a dynamical system can be parameterized by a differential equation,

$$\dot{\boldsymbol{x}} = \boldsymbol{f}(\boldsymbol{x}, \boldsymbol{u}, t; \boldsymbol{p}) \qquad (1)$$

where, $\boldsymbol{p} \in supp(\boldsymbol{p}) \subseteq \mathbb{R}^{N_p}$ is an N_p-dimensional uncertain parameter defined over a support $supp(\boldsymbol{p})$ such that $\boldsymbol{f} : (\boldsymbol{x}, \boldsymbol{u}, t, \boldsymbol{p}) \mapsto \mathbb{R}^{N_x}$ is deterministic if $\boldsymbol{p}$ is known. Throughout this paper we assume all data functions are differentiable. Given any deterministic control trajectory $t \mapsto \boldsymbol{u}$, the evolution of a state trajectory $t \mapsto \boldsymbol{x}$ governed by (1) is deterministically conditioned on the knowledge of $\boldsymbol{p}$. Because $\boldsymbol{p}$ is unknown, we treat (1) as a deterministic selection of a controlled differential inclusion,

$$\dot{\boldsymbol{x}} \in \mathcal{F}(\boldsymbol{x}, \boldsymbol{u}, t) := \{\boldsymbol{f}(\boldsymbol{x}, \boldsymbol{u}, t; \boldsymbol{p}) : \boldsymbol{p} \in supp(\boldsymbol{p})\} \qquad (2)$$

Hence, for a given control trajectory, (1) or (2) emit set-valued states from a known initial state as illustrated in Fig. 1. Such dynamical systems have found widespread applications in aerospace engineering [1]–[3], [13], search theory [14]–[16], and quantum control [17], [18] to name

I. M. Ross is a Professor and Program Director of Control and Optimization at the Naval Postgraduate School, Monterey, CA 93943 USA.

M. Karpenko is a Research Associate Professor of Control and Optimization at the Naval Postgraduate School, Monterey, CA 93943 USA. mkarpenk@nps.edu

R. J. Proulx is a Research Professor of Control and Optimization at the Naval Postgraduate School, Monterey, CA 93943 USA.
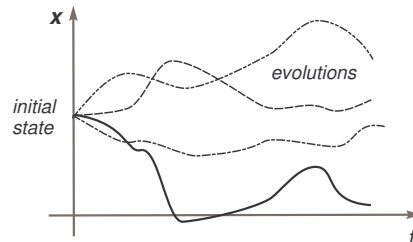

Fig. 1. The evolution of a state trajectory is set-valued for (1) or (2) for any given control trajectory; figure adapted from Aubin et al [12].

a few. It has also been widely studied in the Russian literature [19] and has led to a minimax or robust optimal control theory as put forth separately by Vinter [20] and Boltyanski and Poznyak [21]. Because (1) is not a stochastic differential equation, that is, an Itô differential equation with a diffusion term, it is called a tychastic differential equation, after *Tyche*, the ancient Greek goddess of chance and fortune [12], [22]. By using the unscented transform [6] to map the mean and covariance of $\boldsymbol{p}$ to a collection of sigma points, a tychastic optimal control problem maps to an unscented optimal control problem [2]. The unscented optimal control problem is deterministic but possibly large scale; hence, the spectral efficiencies of pseudospectral optimal control techniques [23] are a good match to solve these problems. In both the simulations and the experimental implementations presented later in this paper, we used the MATLAB® toolkit DIDO©[1] which implements the spectral algorithm [24], [25] for solving optimal control problems. In general, an unscented optimal control solves the original tychastic problem approximately [3]. Hence, it can be viewed as solving an associated chance-constrained optimal control problem exactly. In this case, the risk level is determined a posteriori by a Monte Carlo simulation [3], [5]. These ideas have found new applications in aerospace engineering such as in extending the life of the Hubble space telescope [1] and providing safety margins for spacecraft proximity operations over distant asteroids [2].

In this paper, we further these emerging concepts by incorporating path constraints in the problem formulation. That is, in nearly all of the prior work, the state space was an open set. In many engineering applications it is critical to incorporate collision avoidance constraints, keep-out zones, and other physical and operational constraints. General deterministic path constraints impose restrictions on $\big(\boldsymbol{x}(\cdot), \boldsymbol{u}(\cdot)\big)$

by means of functional constraints, $\boldsymbol{h}(\boldsymbol{x}(t), \boldsymbol{u}(t)) \leq \boldsymbol{0} \,\forall\, t \in [t_0, t_f]$ where, $\boldsymbol{h} : \mathbb{R}^{N_x} \times \mathbb{R}^{N_u} \to \mathbb{R}^{N_h}$ is a given function. In this paper, we incorporate a tychastic version of such path constraints and extend a minimum principle. In addition, we incorporate uncertainties in the initial state vector, $\boldsymbol{x}^0$. Uncertainty in the initial value of the state vector is particularly important in interplanetary space operations where the initial conditions may be derived from an imprecisely targeted condition of a preceding phase in a mission plan. For instance, during the landing phase of a distant celestial body (e.g., asteroid) the initial conditions are derived from the targeting conditions of a prior phase of injection.

II. DEVELOPMENT OF A PROBLEM FORMULATION

In this paper, we consider uncertainties in the initial state. Uncertainties in the dynamical system are implicitly incorporated in such a formulation through the addition of an integrator [4]. For similar reasons we consider "autonomous" dynamical systems.

In many practical systems, the components of a state vector are not independent. For example, the variables of a quaternion that parameterizes the orientation of a spacecraft must lie on S^3. Hence, we need to consider conditionally dependent uncertain variables. These requirements from practical considerations can be articulated as

$$\boldsymbol{x}^0 \equiv \boldsymbol{p} \in supp(\boldsymbol{p}) \quad \text{and} \quad \boldsymbol{e}_0(\boldsymbol{x}^0) \leq \boldsymbol{0} \qquad (3)$$

where, $\boldsymbol{e}_0 : \mathbb{R}^{N_x} \to \mathbb{R}^{N_{e0}}$ is a given function. Hence, we consider uncertain initial states that satisfy the condition,

$$\boldsymbol{x}^0 \in \mathbb{E}_0 := \big\{ \boldsymbol{p} \in \mathbb{R}^{N_x} : \boldsymbol{e}_0(\boldsymbol{p}) \leq \boldsymbol{0} \,\forall\, \boldsymbol{p} \in supp(\boldsymbol{p}) \big\} \quad (4)$$

Given a deterministic control trajectory $t \mapsto \boldsymbol{u} \in \mathbb{U} \subseteq \mathbb{R}^{N_u}$ and a deterministic dynamical system,

$$\dot{\boldsymbol{x}} = \boldsymbol{f}(\boldsymbol{x}, \boldsymbol{u}) \qquad (5)$$

the evolution of $\boldsymbol{x}$ is uncertain with uncertain initial conditions; see Fig. 2. At any given time t, the cross-section of
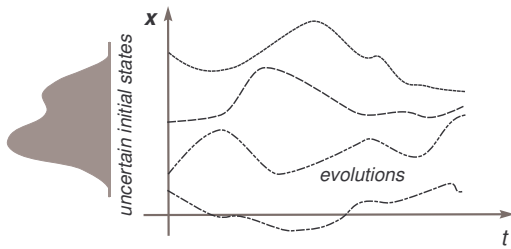

Fig. 2. Set-valued evolutions of a state trajectory for uncertain initial conditions. Compare with Fig. 1.

the evolution is given by the set $\{\boldsymbol{x}(t, \boldsymbol{p}) : \boldsymbol{p} \in supp(\boldsymbol{p})\}$ where, $t \mapsto \boldsymbol{x}(t, \boldsymbol{p})$ is a parameterized absolutely-continuous solution to (5) (for a given control trajectory $t \mapsto \boldsymbol{u}$).

Suppose we are given a target set,

$$\big\{ \boldsymbol{x}_f \in \mathbb{R}^{N_x} : \boldsymbol{e}_f(\boldsymbol{x}_f) \leq \boldsymbol{0} \big\} \qquad (6)$$

where, $\boldsymbol{e}_f : \mathbb{R}^{N_x} \to \mathbb{R}^{N_{ef}}$ is a given function. In a tychastic optimal control problem, the objective is to find

a deterministic control trajectory that drives the initial set $\{\boldsymbol{x}(t_0, \boldsymbol{p}) : \boldsymbol{p} \in supp(\boldsymbol{p})\}$ to the target set while minimizing a given cost functional,

$$J : \big(\boldsymbol{x}(\cdot, \cdot), \boldsymbol{u}(\cdot)\big) \mapsto \mathbb{R} \qquad (7)$$

In minimax or robust optimal control [20], [21], the cost functional is given by

$$J[\boldsymbol{x}(\cdot, \cdot), \boldsymbol{u}(\cdot)] := \max_{\boldsymbol{p} \in supp(\boldsymbol{p})} E\big(\boldsymbol{x}(t_f, \boldsymbol{p}), \boldsymbol{p}\big) \qquad (8)$$

where, $E : \mathbb{R}^{N_x} \times \mathbb{R}^{N_x} \to \mathbb{R}$ is a given function. The caveats in (8) are that $supp(\boldsymbol{p})$ be compact and the initial condition be deterministic. As indicated in [1]–[5], [11], in many engineering applications there is a need to consider alternative cost criteria that include the important case of minimum time problems. To this end, we consider Lebesgue-Stieltjes cost functionals given by

$$J[\boldsymbol{x}(\cdot, \cdot), \boldsymbol{u}(\cdot)] := \int_{supp(\boldsymbol{p})} E\big(\boldsymbol{x}(t_f, \boldsymbol{p}), \boldsymbol{p}\big) \, dm(\boldsymbol{p}) \qquad (9)$$

where, $m : \boldsymbol{p} \mapsto \mathbb{R}_+$ is a measure function given by the cumulative distribution function (CDF) of $\boldsymbol{p}$. Furthermore, we allow the initial set and final set to be jointly dependent and hence consider general boundary conditions of the form,

$$\boldsymbol{e}(\boldsymbol{x}(t_f, \boldsymbol{p}), \boldsymbol{p}) \leq \boldsymbol{0} \quad \forall\, \boldsymbol{p} \in supp(\boldsymbol{p}) \qquad (10)$$

where $\boldsymbol{e} : \mathbb{R}^{N_x} \times \mathbb{R}^{N_x} \to \mathbb{R}^{N_e}$ is a given data function. More importantly, we also consider mixed state-control path constraints given by

$$\boldsymbol{h}(\boldsymbol{x}(t, \boldsymbol{p}), \boldsymbol{u}(t)) \leq \boldsymbol{0} \quad \forall\, (t, \boldsymbol{p}) \in [t_0, t_f] \times supp(\boldsymbol{p}) \quad (11)$$

where, $\boldsymbol{h} : \mathbb{R}^{N_x} \times \mathbb{R}^{N_u} \to \mathbb{R}^{N_h}$ is a given function. Collecting all the relevant equations, we formulate a transcendental tychastic optimal control problem as:

$$\boldsymbol{x} \in \mathbb{R}^{N_x}, \quad \boldsymbol{u} \in \mathbb{U} \subseteq \mathbb{R}^{N_u}, \quad \boldsymbol{x}(t_0, \boldsymbol{p}) \equiv \boldsymbol{p} \in supp(\boldsymbol{p})$$

$$(LS^\infty) \begin{cases} \text{Minimize } J[\boldsymbol{x}(\cdot, \cdot), \boldsymbol{u}(\cdot)] := \\ \qquad \int_{supp(\boldsymbol{p})} E\big(\boldsymbol{x}(t_f, \boldsymbol{p}), \boldsymbol{p}\big) \, dm(\boldsymbol{p}) \\ \text{Subject to } \dot{\boldsymbol{x}}(t, \boldsymbol{p}) = \boldsymbol{f}(\boldsymbol{x}(t, \boldsymbol{p}), \boldsymbol{u}(t)) \\ \qquad \boldsymbol{e}(\boldsymbol{x}(t_f, \boldsymbol{p}), \boldsymbol{p}) \leq \boldsymbol{0} \\ \qquad \boldsymbol{h}(\boldsymbol{x}(t, \boldsymbol{p}), \boldsymbol{u}(t)) \leq \boldsymbol{0} \end{cases}$$

where, barring the usual technicalities of zero measures, all constraints are required to be satisfied for all $t \in [t_0, t_f]$ and all $\boldsymbol{p} \in supp(\boldsymbol{p})$. Note also that we allow abstract constraints on the control variable ($\boldsymbol{u} \in \mathbb{U}$ in the preamble) in addition to the path constraints as proposed by Dubovitskii and Milyutin [11], [26]. It will be apparent in Sections V and VI that all these generalities are indeed essential for practical problem solving.

The existence of a solution to Problem LS^∞ is the main problem in tychastic optimal control theory [2], [11]. From a practical perspective, it can be addressed to some extent through the use of unscented techniques as discussed in the next section.

III. UNSCENTED OPTIMAL CONTROL

In this section we briefly review unscented optimal control [1]–[3] with the addition of a path constraint. Later, in Section IV, we will connect it to Problem LS^∞ as its low-order semi-discrete version.

Let $\boldsymbol{\mu}_{x^0}$ and $\boldsymbol{\Sigma}_{x^0}$ be the mean and covariance of $\boldsymbol{x}(t_0, \boldsymbol{p}) \equiv \boldsymbol{p}$. Then it is quite straightforward [7], [9] to determine a set of sigma points $\boldsymbol{\chi}_1^0, \boldsymbol{\chi}_2^0, \ldots, \boldsymbol{\chi}_{N_\sigma}^0$ at $t = t^0$. The dynamics of each sigma point, $\boldsymbol{\chi}_i, i = 1, \ldots, N_\sigma$ is given by $\dot{\boldsymbol{\chi}}_i = \boldsymbol{f}(\boldsymbol{\chi}_i, \boldsymbol{u}, t)$. Let $\boldsymbol{X}$ be an $N_\sigma N_x$-dimensional vector given by,

$$\boldsymbol{X} := (\boldsymbol{\chi}_1, \boldsymbol{\chi}_2, \ldots, \boldsymbol{\chi}_{N_\sigma}) \in \mathbb{R}^{N_\sigma N_x}$$

The dynamics of $\boldsymbol{X}$ are simply N_σ copies of $\boldsymbol{f}$ given by

$$\dot{\boldsymbol{X}} = (\boldsymbol{f}(\boldsymbol{\chi}_1, \boldsymbol{u}, t), \ldots, \boldsymbol{f}(\boldsymbol{\chi}_{N_\sigma}, \boldsymbol{u}, t)) := \boldsymbol{F}(\boldsymbol{X}, \boldsymbol{u}, t)$$

In unscented optimal control, we consider the controlled dynamical system $\dot{\boldsymbol{X}} = \boldsymbol{F}(\boldsymbol{X}, \boldsymbol{u}, t)$, whose initial state is given by the sigma points

$$\boldsymbol{X}(t_0) = \boldsymbol{X}^0 := (\boldsymbol{\chi}_1^0, \boldsymbol{\chi}_2^0, \ldots \boldsymbol{\chi}_{N_\sigma}^0)$$

The objective is to find a control trajectory $t \mapsto \boldsymbol{u}$ that that drives $\boldsymbol{X}^0$ to a target state while minimizing a cost functional and satisfying the path constraints. Thus, an unscented optimal control problem can be framed as the following deterministic optimal control problem:

$$\boldsymbol{X} \in \mathbb{X}^{N_\sigma} = \mathbb{R}^{N_\sigma N_x}, \quad \boldsymbol{u} \in \mathbb{U} \subseteq \mathbb{R}^{N_u}$$

$$(U) \begin{cases} \text{Minimize} & J[\boldsymbol{X}(\cdot), \boldsymbol{u}(\cdot)] := E(\boldsymbol{X}(t_f), \boldsymbol{X}(t_0)) \\ \text{Subject to} & \dot{\boldsymbol{X}}(t) = \boldsymbol{F}(\boldsymbol{X}(t), \boldsymbol{u}(t)) \\ & \boldsymbol{e}(\boldsymbol{X}(t_f), \boldsymbol{X}(t_0)) \leq \boldsymbol{0} \\ & \boldsymbol{h}(\boldsymbol{X}(t), \boldsymbol{u}(t)) \leq \boldsymbol{0} \end{cases}$$

where, for the purposes of economy of notation, we have reused the symbols $E, \boldsymbol{e}$, and $\boldsymbol{h}$ to mean the same concepts as before but with different sets of inputs and outputs: $E : \mathbb{X}^{N_\sigma} \times \mathbb{X}^{N_\sigma} \to \mathbb{R}$, $\boldsymbol{e} : \mathbb{X}^{N_\sigma} \times \mathbb{X}^{N_\sigma} \to \mathbb{R}^{N_e}$, and $\boldsymbol{h} : \mathbb{X}^{N_\sigma} \times \mathbb{U} \to \mathbb{R}^{N_h}$.

Through the use of engineering principles, it is possible to frame a sequence of unscented optimal control problems that numerically approach a solution to Problem LS^∞ [1], [2]; however, the most that can be guaranteed from a mathematical perspective is the satisfaction of the transcendental constraints in the mean and covariances (and possibly a few more higher-order moments depending upon the choice of the sigma points). In any case, once an unscented control is obtained, a Monte Carlo simulation may be performed to estimate the risk levels,

$$\widetilde{r}_e := 1 - Pr\{\boldsymbol{e}(\boldsymbol{x}(t_f, \boldsymbol{p}), \boldsymbol{p}) \leq \boldsymbol{0}\} \tag{12}$$

$$\widetilde{r}_h := \max_{t \in [t_0, t_f]} (1 - Pr\{\boldsymbol{h}(\boldsymbol{x}(t, \boldsymbol{p}), \boldsymbol{u}(t)) \leq \boldsymbol{0}\}) \tag{13}$$

where $Pr\{A\}$ denotes the probability of event A. Thus, the unscented control solves the chance-constrained optimal control problem,

$$\boldsymbol{x} \in \mathbb{R}^{N_x}, \quad \boldsymbol{u} \in \mathbb{R}^{N_u}, \quad \boldsymbol{x}(t_0, \boldsymbol{p}) \equiv \boldsymbol{p} \in supp(\boldsymbol{p})$$

$$(C) \begin{cases} \text{Minimize } J[\boldsymbol{x}(\cdot, \cdot), \boldsymbol{u}(\cdot)] := \\ \qquad \int_{supp(\boldsymbol{p})} E(\boldsymbol{x}(t_f, \boldsymbol{p}), \boldsymbol{p}) \, dm(\boldsymbol{p}) \\ \text{Subject to } \dot{\boldsymbol{x}}(t, \boldsymbol{p}) = \boldsymbol{f}(\boldsymbol{x}(t, \boldsymbol{p}), \boldsymbol{u}(t)) \\ \qquad Pr\{\boldsymbol{e}(\boldsymbol{x}(t_f, \boldsymbol{p}), \boldsymbol{p}) \leq \boldsymbol{0}\} \geq 1 - r_e \\ \qquad \max_{t \in [t_0, t_f]} Pr\{\boldsymbol{h}(\boldsymbol{x}(t, \boldsymbol{p}), \boldsymbol{u}(t)) \leq \boldsymbol{0}\} \\ \qquad\qquad\qquad\qquad \geq 1 - r_h \end{cases}$$

where r_e and r_h are the risk levels associated with the targeted condition and the path-constraint satisfaction respectively.

In the next section, we provide another perspective for Problem U as a low-order semi-discretization of the transcendental tychastic optimal control problem.

IV. THEORETICAL FOUNDATIONS

A minimum principle for the transcendental tychastic optimal control problem can be obtained by an application of the generalized covector mapping principle [4], [11]. In this approach, the necessary conditions are derived by taking the limits of a semi-discretization. To this end, consider any (convergent) cubature scheme that approximates the Lebesgue-Stieltjes cost functional given in Problem LS^∞. That is, let $(\boldsymbol{p}_i, w_i)$ $i = 1, \ldots, n$ be a collection of nodes and nonnegative weights such that

$$\int_{supp(\boldsymbol{p})} E(\boldsymbol{x}(t_f, \boldsymbol{p}), \boldsymbol{p}) \, dm(\boldsymbol{p}) =$$

$$\lim_{n \to \infty} \sum_{i=1}^n w_i E(\boldsymbol{x}(t_f, \boldsymbol{p}_i), \boldsymbol{p}_i)$$

Then, for any finite n, we can semi-discretize Problem LS^∞ as:

$$\boldsymbol{x}_i \in \mathbb{R}^{N_x}, \quad \boldsymbol{u} \in \mathbb{U} \subseteq \mathbb{R}^{N_u}, \quad \boldsymbol{x}_i(t_0) \equiv \boldsymbol{p}_i \in supp(\boldsymbol{p})$$

$$i = 1, \ldots, n$$

$$(LS^n) \begin{cases} \text{Minimize } J[\boldsymbol{x}_1(\cdot), \ldots \boldsymbol{x}_n(\cdot), \boldsymbol{u}(\cdot)] := \\ \qquad\qquad \sum_{i=1}^n w_i E(\boldsymbol{x}_i(t_f), \boldsymbol{p}_i) \\ \text{Subject to } \dot{\boldsymbol{x}}_1(t) = \boldsymbol{f}(\boldsymbol{x}_1(t), \boldsymbol{u}(t)) \\ \qquad\qquad \vdots \\ \qquad \dot{\boldsymbol{x}}_n(t) = \boldsymbol{f}(\boldsymbol{x}_n(t), \boldsymbol{u}(t)) \\ \qquad \boldsymbol{e}(\boldsymbol{x}_1(t_f), \boldsymbol{p}_1) \leq \boldsymbol{0} \\ \qquad\qquad \vdots \\ \qquad \boldsymbol{e}(\boldsymbol{x}_n(t_f), \boldsymbol{p}_n) \leq \boldsymbol{0} \\ \qquad \boldsymbol{h}(\boldsymbol{x}_1(t), \boldsymbol{u}(t)) \leq \boldsymbol{0} \\ \qquad\qquad \vdots \\ \qquad \boldsymbol{h}(\boldsymbol{x}_n(t), \boldsymbol{u}(t)) \leq \boldsymbol{0} \end{cases}$$

The consistency of a version of Problem LS^n with respect to Problem LS^∞ is proved in [16]. Motivated by the theoretical components of our prior work [2]–[5], we write the Hamiltonian for Problem LS^n as

$$\widetilde{I}(\widetilde{\boldsymbol{\lambda}}_1,\ldots,\widetilde{\boldsymbol{\lambda}}_n,\boldsymbol{x}_1,\ldots,\boldsymbol{x}_n,\boldsymbol{u}) := \sum_{i=1}^n w_i\, H\left(\frac{\widetilde{\boldsymbol{\lambda}}_i}{w_i},\boldsymbol{x}_i,\boldsymbol{u}\right) \quad (14)$$

where, $\widetilde{\boldsymbol{\lambda}}_i \in \mathbb{R}^{N_x}, i = 1,\ldots,n$ are the adjoint covectors, and H is the Pontryagin Hamiltonian function

$$H(\boldsymbol{\lambda},\boldsymbol{x},\boldsymbol{u}) := \boldsymbol{\lambda}^T \boldsymbol{f}(\boldsymbol{x},\boldsymbol{u}) \quad (15)$$

Taking the limit of (14) we define the integrated Hamiltonian functional as

$$I(\boldsymbol{\lambda}(t,\cdot),\boldsymbol{x}(t,\cdot),\boldsymbol{u}) := \int_{supp(\boldsymbol{p})} H(\boldsymbol{\lambda}(t,\boldsymbol{p}),\boldsymbol{x}(t,\boldsymbol{p}),\boldsymbol{u})\, dm(\boldsymbol{p}) \quad (16)$$

where, $t \mapsto \boldsymbol{\lambda}(t,\boldsymbol{p}) \in \mathbb{R}^{N_x}$ is a covector function for each $\boldsymbol{p}$ that satisfies the adjoint differential equation

$$-\dot{\boldsymbol{\lambda}}(t,\boldsymbol{p}) = \partial_{\boldsymbol{x}}\overline{H}\big(\boldsymbol{\mu}(t,\boldsymbol{p}),\boldsymbol{\lambda}(t,\boldsymbol{p}),\boldsymbol{x},\boldsymbol{u}(t)\big)\Big|_{\boldsymbol{x}=\boldsymbol{x}(t,\boldsymbol{p})} \quad (17)$$

$\overline{H}$ is the Lagrangian of the Hamiltonian [11] defined as

$$\overline{H}(\boldsymbol{\mu},\boldsymbol{\lambda},\boldsymbol{x},\boldsymbol{u}) := H(\boldsymbol{\lambda},\boldsymbol{x},\boldsymbol{u}) + \boldsymbol{\mu}^T \boldsymbol{h}(\boldsymbol{x},\boldsymbol{u}) \quad (18)$$

and $t \mapsto \boldsymbol{\mu}(t,\boldsymbol{p}) \in \mathbb{R}^{N_h}$ is the path covector function associated with (11) that satisfies the complementarity condition,

$$\boldsymbol{0} \le \boldsymbol{\mu}(t,\boldsymbol{p}) \perp \boldsymbol{h}(\boldsymbol{x}(t,\boldsymbol{p}),\boldsymbol{u}(t)) \le \boldsymbol{0} \quad \forall\, \boldsymbol{p} \in supp(\boldsymbol{p}) \quad (19)$$

Thus, the optimal control satisfies the the integrated Hamiltonian minimization condition (iHMC)

$$\text{(iHMC)} \begin{cases} \underset{\boldsymbol{u}(t)}{\text{Min}} & I[\boldsymbol{\lambda}(t,\cdot),\boldsymbol{x}(t,\cdot),\boldsymbol{u}(t)] := \\ & \int_{supp(\boldsymbol{p})} H(\boldsymbol{\lambda}(t,\boldsymbol{p}),\boldsymbol{x}(t,\boldsymbol{p}),\boldsymbol{u}(t))\, dm(\boldsymbol{p}) \\ \text{s. t.} & \boldsymbol{h}(\boldsymbol{x}(t,\boldsymbol{p}),\boldsymbol{u}(t)) \le \boldsymbol{0} \quad \forall\, \boldsymbol{p} \in supp(\boldsymbol{p}) \\ & \boldsymbol{u}(t) \in \mathbb{U} \end{cases}$$

Although it resembles one, Problem iHMC is not exactly a classic semi-infinite programming problem; however, it is indeed an instantaneous transcendental (static) optimization problem considered in [27]. Consequently, we may use the recent results of unscented programming [27] to analyze Problem iHMC.

Following the same procedure, it follows that the transversality condition is given by

$$\boldsymbol{\lambda}(t_f,\boldsymbol{p}) = \frac{\partial \overline{E}(\boldsymbol{\nu},\boldsymbol{x}_f,\boldsymbol{p})}{\partial \boldsymbol{x}_f}\Bigg|_{(\boldsymbol{\nu}(\boldsymbol{p}),\boldsymbol{x}(t_f,\boldsymbol{p}),\boldsymbol{p})} \quad (20)$$

where, $\overline{E} : \mathbb{R}^{N_e} \times \mathbb{R}^{N_x} \times \mathbb{R}^{N_x} \to \mathbb{R}$ is the endpoint Lagrangian

$$\overline{E}(\boldsymbol{\nu},\boldsymbol{x}_f,\boldsymbol{p}) := E(\boldsymbol{x}_f,\boldsymbol{p}) + \boldsymbol{\nu}^T \boldsymbol{e}(\boldsymbol{x}_f,\boldsymbol{p})$$

and $\boldsymbol{\nu} : \boldsymbol{p} \mapsto \mathbb{R}^{N_e}$ in (20) is an endpoint covector function that is complementary to $\boldsymbol{e}$ in an analogous manner as (19).

When path constraints are added to even a deterministic optimal control problem, it requires an entirely new set of mathematical machinery to accommodate for atomic measures that naturally enter in the construction of the multiplier rule [10], [11]. It is therefore not surprising that these issues carry over to tychastic optimal control problems as well. For the purposes of brevity, we omit these details while noting that the adjoint covector function $t \mapsto \boldsymbol{\lambda}(t,\boldsymbol{p})$ may exhibit jumps. These jump conditions can be directly connected to the properties of the path covector function $t \mapsto \boldsymbol{\mu}(t,\boldsymbol{p})$ as discussed in [11].

V. A SPACE APPLICATION PROBLEM

The use of satellite imagery is ubiquitous: from an everyday map application in a smart phone to providing timely agricultural soil information to a farmer. In order to meet the increasing demands, a satellite is required to point and re-point rapidly and accurately [28]. The dynamics of an agile spacecraft are given by [29],

$$\dot{\boldsymbol{q}} = \tfrac{1}{2}\mathbf{Q}(\boldsymbol{\omega})\mathbf{q}$$
$$\dot{\boldsymbol{\omega}} = \mathbf{I}^{-1}\big(-\boldsymbol{\omega} \times \mathbf{I} \cdot \boldsymbol{\omega} - \boldsymbol{\omega} \times \mathbf{h}_c(\boldsymbol{\delta}) - \mathbf{A}(\boldsymbol{\delta})\mathbf{u}\big)$$
$$\dot{\boldsymbol{\delta}} = \mathbf{u}$$

where, $\boldsymbol{q} \in \mathbb{R}^4$ is a quaternion that parameterizes its attitude in inertial space, $\boldsymbol{\omega} \in \mathbb{R}^3$ is the body rate, $\boldsymbol{\delta}$ is an N_c-vector of gimbal angles associated with the onboard control moment gyros (CMGs), $\mathbf{I}$ is the inertia matrix of the spacecraft, $\boldsymbol{h}_c(\boldsymbol{\delta})$ is the angular momentum of the CMG configuration, and $\boldsymbol{A}(\boldsymbol{\delta})$ is a $3 \times N_c$ effector matrix associated with the control vector $\boldsymbol{u} \in \mathbb{U} \subset \mathbb{R}^{N_c}$ of gimbal rates.

Any time a spacecraft is not collecting imagery is considered wasted time and lost revenue; hence, our primary objective is to minimize the time to maneuver between two collects. This commercial objective can be mathematically translated to a canonical optimal control problem as:

$$J_{com}[\boldsymbol{x}(\cdot),\boldsymbol{u}(\cdot),t_f] := t_f$$
$$\boldsymbol{q}(0) = \boldsymbol{q}^0, \quad \boldsymbol{q}(t_f) = \boldsymbol{q}^f$$
$$\boldsymbol{\omega}(0) = \boldsymbol{\omega}^0, \quad \boldsymbol{\omega}(t_f) = \boldsymbol{\omega}^f$$
$$\boldsymbol{\delta}(0) = \boldsymbol{\delta}^0, \quad \boldsymbol{\delta}(t_f) = \boldsymbol{\delta}^f$$

It is well known [29] that when this problem is solved, it may generate gimbal trajectories $t \mapsto \boldsymbol{\delta}$ that render $\boldsymbol{A}(\boldsymbol{\delta}(t))$ singular at some $t \in [t_0,t_f]$. This essentially makes the spacecraft uncontrollable; hence, to avoid this singularity we impose a path constraint,

$$t \mapsto S(\boldsymbol{\delta}) := \sqrt{\det\big[\boldsymbol{A}(\boldsymbol{\delta})\boldsymbol{A}^T(\boldsymbol{\delta})\big]} \ge S_{margin} \forall\, t \in [t_0,t_f]$$

where $S_{margin} > 0$ is an engineering decision. For a box configuration of four CMGs [30], [31], $\boldsymbol{A}(\boldsymbol{\delta})$ is given by

$$\boldsymbol{A}(\boldsymbol{\delta}) := \begin{bmatrix} 0 & \sin(\delta_2) & 0 & -\sin(\delta_4) \\ \cos(\delta_1) & \cos(\delta_2) & \cos(\delta_3) & \cos(\delta_4) \\ \sin(\delta_1) & 0 & -\sin(\delta_3) & 0 \end{bmatrix}$$

A plot of the path constraint function $t \mapsto S(\boldsymbol{\delta}(t))$ for this deterministic optimal control problem is shown in Fig. 3. For the purposes of brevity, only key plots are presented.
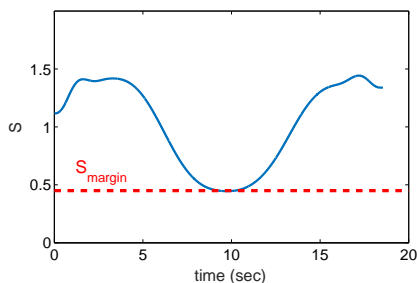

Fig. 3. A minimum-time path-constrained control solution to the spacecraft attitude steering problem indicates the satisfaction of the safety constraint.

All results were generated using DIDO$^{©}$ [11]. The DIDO results were verified and validated using standard procedures discussed in detail in [11].

In a practical implementation, $\boldsymbol{q}$ and $\boldsymbol{\omega}$ at the boundary points are dictated from the precise requirements for satellite imagery. Although there are no targeting requirements on $\boldsymbol{\delta}$, its initial value is determined by the final value of the gimbal position from the previously imaged condition. This quantity is not known precisely because it is implemented as an inner loop in a feedback control system. By setting $\boldsymbol{\delta}^0 = \boldsymbol{p}$ as an uncertain parameter, we can numerically test the optimal slew profile for robustness in its singularity avoidance. We assume $\boldsymbol{\delta}^0$ to be uncorrelated Gaussian with standard deviation $\sigma = 10^o$. A Monte Carlo simulation shows that (see Fig. 4) the path constraints $S(\boldsymbol{\delta}(t)) \geq S_{margin}$ is violated
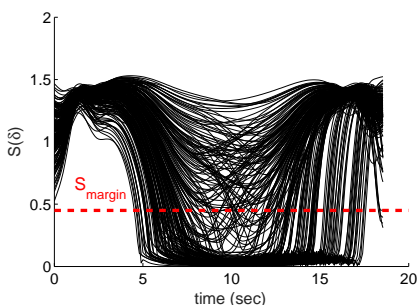

Fig. 4. Monte Carlo simulation results for deterministic control indicates a violation of the path constraint that cross the safety margin that includes the failure zone of $S(\delta(t)) = 0$.

quite often. Furthermore, this violation is quite severe in many cases as evident by the many samples in Fig. 4 where $S(\boldsymbol{\delta}(t))$ is zero. In the absence of an experimental test, we do not know how many of our assumptions are valid; hence, we now present these results.

VI. EXPERIMENTAL RESULTS

To support the increasing business of agile spacecraft, Honeywell has set up a state-of-the-art test facility in Phoenix, AZ; see Fig. 5. Through a partnership program with
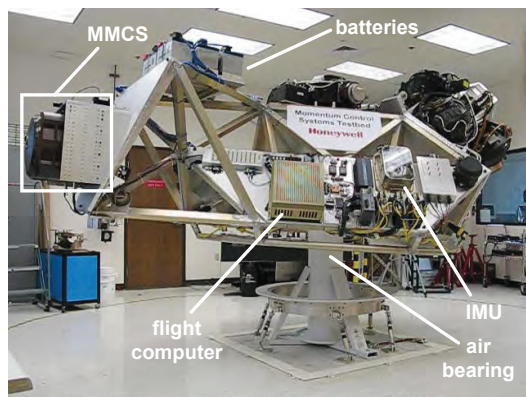

Fig. 5. Honeywell's ground test facility where several experiments on unscented optimal control were conducted in an operationally-relevant environment.

the U.S. Air Force Research Laboratory we conducted a large number of tests on various control schemes and architectures over an operationally relevant scenario. We use the results from one of these tests to illustrate the theory.

An experimental implementation of the deterministic control shown in Fig. 3 resulted in a failure. This is not entirely surprising from the perspective of the pre-test Monte Carlo simulations of Fig. 4.

We now develop a path-constrained tychastic optimal problem by imposing the transcendental constraint,

$$S\big(\boldsymbol{\delta}(t, \boldsymbol{\delta}^0)\big) \geq S_{margin} \quad \forall\, (t, \boldsymbol{\delta}^0) \in [t_0, t_f] \times supp(\boldsymbol{\delta}^0)$$

while continuing to demand minimum-time performance,

$$J[\boldsymbol{x}(\cdot, \cdot), \boldsymbol{u}(\cdot), t_f] := \int_{supp(\delta^0)} t_f \, \mathrm{d}m(\boldsymbol{\delta}^0) \quad = \; t_f \quad (21)$$

Equation (21) shows that standard cost functionals are naturally allowed in the tychastic formulation. The unscented implementation (transcendental form) is given by

$$S\big(\boldsymbol{\delta}(t, \boldsymbol{\delta}_1^0)\big) \geq S_{margin}$$
$$\vdots \qquad\qquad \forall\, t \in [t_0, t_f]$$
$$S\big(\boldsymbol{\delta}(t, \boldsymbol{\delta}_{N_\sigma}^0)\big) \geq S_{margin}$$

where $\boldsymbol{\delta}_1^0, \dots \boldsymbol{\delta}_{N_\sigma}^0$ are the sigma points of $\boldsymbol{\delta}^0$. A Monte Carlo simulation (see Fig. 6) shows that the performance of the unscented optimal control is drastically different from that of the deterministic optimal control. That is, the path constraints are not violated for the majority of the samples and even when they cross the safety margin, the values of $S(\boldsymbol{\delta}(t))$ remain above the failure zone (zero).

An experimental implementation of the unscented control was successful over all trials conducted. These results are shown in Fig. 7. Note in particular that one of the experimental trials is even outside of the Monte Carlo tube of Fig. 6.

VII. CONCLUSIONS

When uncertainty is managed in a practical implementation through the use of feedback control, standard optimal
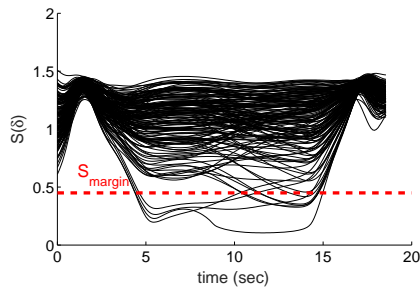
Fig. 6. Monte Carlo results for the unscented control shows a significant improvement in safety. Compare to Fig. 4.
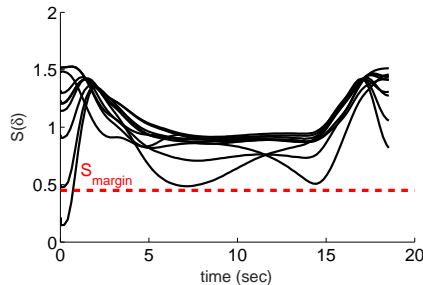

Fig. 7. Experimental results of the unscented optimal control conducted at Honeywell showed that all trials were successful.

controls may not be desirable because they might put the system in uncontrollable regions. By explicitly incorporating system uncertainties in an optimal control framework we arrive at a tychastic problem formulation. The computational challenges in solving a tychastic optimal control problem are immense; however, the unscented transform offers a simple way out through its use of sigma points. The price for this simplicity is a solution to a chance-constrained optimal control problem whose risk is determined a posteriori through the use of a Monte Carlo simulation. Successful experimental results validate the need for an entirely new area of research where a large number of open problems in theory and computation need to be addressed.

ACKNOWLEDGMENTS

REFERENCES

[1] Ross, I. M., Proulx, R. J., and Karpenko, M., "Unscented Optimal Control For Space Flight," *24th International Symp. on Space Flight Dynamics (ISSFD)*, Laurel, MD, May 5-9, 2014.

[2] Ross, I. M., Proulx, R. J., and Karpenko, M., "Unscented Optimal Control for Orbital and Proximity Operations in an Uncertain Environment: A New Zermelo Problem," *AIAA Space and Astro. Forum and Expo.: AIAA/AAS Astrodynamics Specialist Conf.*, San Diego, CA 4-7 August 2014.

[3] Ross, I. M., Proulx, R. J., and Karpenko, M. "Unscented Guidance," *Proceedings of the ACC*, Chicago, IL, July 1–3, 2015.

[4] Ross, I. M., Proulx, R. J., Karpenko M. and Gong, Q., "Riemann-Stieltjes Optimal Control Problems for Uncertain Dynamical Systems," *J. Guid., Control and Dynamics*, Vol. 38, No. 7, 2015, pp. 1251–1263.

[5] Ross, I. M., Karpenko, M. and Proulx, R. J., "A Lebesgue-Stieltjes Framework For Optimal Control and Allocation," *Proceedings of the ACC*, Chicago, IL, July 1–3, 2015.

[6] Julier, S. J. and Uhlmann, J. K., "Unscented Filtering and Nonlinear Estimation," *Proc. of the IEEE* , Vol. 92, No. 3, 2004, pp. 401–422.

[7] Julier, S. J. "The Spherical Simplex Unscented Transformation," *Proc. of the ACC*, Denver, CO, June 4-6, 2003, Vol. 3, pp. 2430–2434.

[8] Julier, S. J. and Uhlmann, J. K., "Reduced Sigma Point Filters for the Propagation of Means and Covriances through Nonlinear Transformations," *Proceedings of the ACC*, Vol. 2, 2002, pp. 887–892.

[9] Julier, S. J., Uhlmann, J. K., and Durrant-Whyte, H. F., "A New Approach for Filtering Nonlinear Systems," *Proceedings of the ACC*, Seattle, WA, 1995, pp. 1628–1632.

[10] Vinter, R. B., *Optimal Control*, Birkhäuser, Boston, MA, 2000.

[11] Ross, I. M. *A Primer on Pontryagin's Principle in Optimal Control*, Second Edition, Collegiate Publishers, San Francisco, CA, 2015.

[12] Aubin, J.-P., Bayen, A. M. and Saint-Pierre, P., *Viability Theory: New Directions*, Second Edition, Springer-Verlag Berlin Heidelberg, 2011.

[13] Shaffer, R., Karpenko, M. and Gong, Q., "Unscented Guidance for Waypoint Navigation of a Fixed-Wing UAV," *Proceedings of the American Control Conference*, Boston, MA, July 6–8, 2016.

[14] Koopman, B. O., "The Theory of Search, I: Target Detection," *Operations Research*, Vol. 4, No. 5, 1956, pp. 503–531.

[15] Stone, L. D. and Richardson, H. R., "Search for Targets with Conditionally Deterministic Motion," *SIAM Journal of Applied Mathematics*, Vol. 27, No. 2, September 1974, pp. 239–255.

[16] Phelps, C., Royset, J. O., and Gong, Q., "Sample Average Approximations in Optimal Control of Uncertain Systems," *Proceedings of the 52nd IEEE CDC*, Florence, Italy, 2013.

[17] Li, J.-S. and Khaneja, N., "Control of Inhomogeneous Quantum Ensembles," *Physical Review A*, Vol. 73, No. 030302(R), 2006, pp. 030302-1–030303-4.

[18] Li, Jr-S., Ruths, J., Yu, T-Y, Arthanari H., and Wagner, G., "Optimal Pulse Design in Quantum Control: A Unified Computational Method," *Proceedings of the NAS*, Vol. 108, No. 5, Feb 2011, pp. 1879-1884.

[19] Kurzhanski, A. B. (Ed), *Advances in Nonlinear Dynamics and Control: A Report from Russia*, Birkhäuser, Boston, 1993.

[20] Vinter, R. B., "Minimax Optimal Control," *SIAM Journal of Control and Optimization*, Vol. 44, No. 3, 2005, pp. 939-968.

[21] Boltyanski, V. G. and Poznyak, A. S., *The Robust Maximum Principle: Theory and Applications*, Birkhäuser, New York, N.Y., 2012.

[22] Aubin, J.-P., Chen, L., Dordan, O., Faleh, A., Lezan, G. and Planchet, F., "Stochastic and Tychastic Approaches to Guaranteed ALM Problem," *Bulletin Français d'Actuariat*, Vol. 12, No. 23, 2012, pp. 59-95.

[23] Ross, I. M. and Karpenko, M. A Review of Pseudospectral Optimal Control: From Theory to Flight, *Annual Reviews in Control*, Vol. 36, No. 2, pp. 182–197, 2012.

[24] Ross, I. M. and Fahroo, F., "Pseudospectral Knotting Methods for Solving Optimal Control Problems," *Journal of Guidance, Control and Dynamics*, Vol. 27, No. 3, pp.397-405, 2004.

[25] Gong, Q., Fahroo, F., and Ross, I. M. "A Spectral Algorithm for Pseudospectral Methods in Optimal Control," *Journal of Guidance, Control and Dynamics*, Vol. 31, No. 3, pp. 460–471, 2008.

[26] Dmitruk, A. V., "On the Development of Pontryagin's Maximum Principle in the Works of A. Ya. Dubovitskii and A. A. Milyutin," *Control and Cybernetics*, Vol. 38, No. 4A, 2009, pp. 923–957.

[27] Ross, I. M., Proulx, R. J. and Karpenko, M., "Unscented Optimization," *AAS/AIAA Astrodynamics Specialist Conference*, Vail, CO, August 9–13, 2015. Paper AAS 015-607.

[28] Ross, I. M., Proulx, R. J., Greenslade, J. M. and Karpenko, M., "Dynamic Optimization for Satellite Image Collection," *AAS/AIAA Space Flight Mechanics Conference*, Napa, CA, February 14–18, 2016. Paper AAS 16-260.

[29] Wie, B., *Space Vehicle Dynamics and Control*, AIAA, Reston, VA, 1998.

[30] McMickell, B., Buchele, P., Gisler, G., and Andrus, J., "Control Moment Gyroscope based Momentum Control Systems in Small Satellites," U.S. Patent US8312782 B2, issued Nov. 20, 2012.

[31] Wise, K. et al., "Guidance, Navigation and Control Applications in the Aerospace Industry: Current Problems and Modern Solutions," *51st IEEE Conference on Decision and Control*, Maui, HI, Dec. 2012.